UDK 691.714:531.755
Original scientific article/Izvirni znanstveni članek

ISSN 1580-2949
Mater. Tehnol.

ANALYSIS OF DUST-PARTICLE EMISSIONS DURING THE CUTTING OF S460 TOOL STEEL

ANALIZA EMISIJ PRAŠNIH DELCEV PRI REZANJU ORODNEGA JEKLA S460

Lovro Cigić[1], Mirza Imširević[2], Milana Ilić Mićunović[3], Sandra Perič[1], Borut Kosec[1,2], Aleš Nagode[1], Damjan Klobčar[2], Blaž Karpe[1*]

[1]Faculty of Natural Sciences and Engineering, University of Ljubljana, Aškerčeva cesta 12, 1000 Ljubljana, Slovenia
[2]Faculty of Mechanical Engineering, University of Ljubljana, Aškerčeva cesta 6, 1000 Ljubljana, Slovenia
[3]Faculty of Technical Sciences, University of Novi Sad, Trg Dositeja Obradovića 6, 21000 Novi Sad, Serbia

Prejem rokopisa – received: 2023-04-20; sprejem za objavo – accepted for publication: 2026-03-18

doi:10.17222/mit.2023.853

Oxyfuel cutting and plasma cutting were investigated with respect to the particulate emissions generated during the cutting of SIHARD S460 cold-work tool steel. The aim of the study was to compare the amount and characteristics of the particles emitted during the two cutting processes. Particles were collected by sampling and analyzed gravimetrically, while their size, morphology, and chemical composition were characterized using FEG-SEM and EDXS. The results indicated that oxyfuel cutting generated higher particulate emissions than plasma cutting, with emission rates of 0.096 g/h and 0.066 g/h, respectively. Oxyfuel cutting produced a higher fraction of particles below 1.75 µm, while particles larger than 5.5 µm were observed only for plasma cutting. All the analyzed particles were smaller than 10 µm. EDXS analysis further revealed that a substantial fraction of the collected particulate matter consisted of metal oxide particles formed during thermal cutting. Overall, oxyfuel cutting was identified as the more intensive source of fine particulate emissions during the processing of SIHARD S460 steel.

Keywords: particulate emissions, S460 tool steel, oxyfuel cutting, plasma cutting

Rezanje s plamenom in rezanje s plazmo sta bila analizirana kot vira emisij trdnih delcev, ki so nastajali pri rezanju orodnega jekla SIHARD S460. Namen raziskave je bil primerjati količino emitiranih trdnih delcev ter njihove značilnosti pri obeh postopkih rezanja. Delci so bili zajeti z osebnim vzorčevalnikom in gravimetrično ovrednoteni, njihova velikost, morfologija in kemijska sestava pa so bile analizirane z metodama FEG-SEM in EDXS. Primerjava obeh postopkov je pokazala, da je bila emisijska stopnja trdnih delcev pri rezanju s plamenom višja kot pri rezanju s plazmo in je znašala 0.096 g/h oziroma 0.066 g/h. Pri rezanju s plamenom je bil zaznan večji delež delcev, manjših od 1.75 µm, medtem ko so bili delci, večji od 5.5 µm, zaznani le pri rezanju s plazmo. Vsi analizirani delci so bili manjši od 10 µm. Analiza EDXS je potrdila, da znaten delež zajetih delcev predstavljajo kovinski oksidi, nastali med toplotnim rezanjem. Rezultati na splošno kažejo, da rezanje s plamenom pri obdelavi jekla SIHARD S460 povzroča več emisij finih trdnih delcev kot rezanje s plazmo.

Ključne besede: emisije delcev, orodno jeklo S460, rezanje s plamenom, rezanje s plazmo

1 INTRODUCTION

Thermal cutting processes are widely used in the metal-fabrication industry, where they enable the efficient separation and shaping of metallic materials. Among them, oxyfuel cutting and plasma cutting are two of the most common technologies. In oxyfuel cutting, the material is locally heated and then cut by an exothermic oxidation reaction, whereas in plasma cutting, material removal is achieved by the action of a high-temperature plasma arc. The selection of the cutting process depends on the material type, thickness, required cut quality and productivity.[1–3]

In addition to their technological importance, both processes are associated with the generation of airborne particulate matter. During thermal cutting, particles are formed by the ejection of molten material as well as by the condensation of metal vapors, which leads to a broad particle-size distribution and different particle morphologies. From the occupational-health perspective, fine particles are of particular concern because they can remain suspended in the working atmosphere and may penetrate deeply into the respiratory tract of exposed operators.[4–7] The risk related to particulate emissions therefore depends not only on the total amount of emitted material, but also on the particle size, particle-size distribution, morphology and chemical composition.

Previous studies have shown that the thermal processing of metals may generate both larger droplets originating from melt ejection and much finer particles formed by vapor condensation. Depending on the process conditions and the material being cut, the emitted particles may contain metallic and non-metallic constituents originating from the base material, surface layers and the thermal cutting process itself. For this reason, the comprehensive characterization of emitted particles is required when assessing operator exposure and the potential health relevance of cutting fumes.[5,6,8–10] Particle char-

*Corresponding author's e-mail:
blaz.karpe@ntf.uni-lj.si (Blaž Karpe)

acterization can be performed using gravimetric and image-analysis methods.[11,12] In addition, scanning electron microscopy combined with energy-dispersive X-ray spectroscopy is a useful approach for examining particle morphology and chemical composition.[13] In accordance with ISO 13322-1, static image analysis enables the determination of particle size and particle-size distribution from captured images of stationary particles.[14]

The present study investigates particulate emissions generated during the oxyfuel and plasma cutting of SIHARD S460 cold-work tool steel. The aim was to compare the amount and characteristics of particles produced by the two cutting processes, with special attention to particle mass, size distribution, morphology, and chemical composition, as these parameters are directly relevant to the assessment of operator exposure during thermal cutting. For this purpose, gravimetric particle sampling, static image analysis, and field-emission scanning electron microscopy combined with EDXS were used, providing complementary information on the mass, size, morphology, and composition of the emitted particulate matter.

2 EXPERIMENTAL PART

The experimental part included the measurement and analysis of particulate emissions generated during the cutting of SIHARD S460 cold-work tool steel. The chemical composition and selected thermal and mechanical properties of the investigated steel are presented in **Table 1** and **Table 2**. The investigated specimens had planar dimensions of 40 mm × 40 mm and a thickness of 10 mm.

Table 1: Chemical composition of S460 tool steel

Element	C	Mn	Cr	Mo	V	Si	Fe
w/%	1.00	0.30	8.00	2.30	0.30	1.10	balance

All the cutting operations and the corresponding particle sampling were performed for 1 min. During each test, particulate emissions were sampled using a ZAMBELLI EGO PLUS TT personal sampler (**Figure 1**), which was calibrated before each measurement. During the measurements, the local extraction device normally used to reduce airborne particulate exposure in the cutting zone was switched off to avoid interference with particle sampling and to enable an assessment of particulate emissions under non-extracted conditions.

Table 2: Thermal and mechanical properties of S460 tool steel at 20 °C

Density	7640 kg/m^3
Specific heat	470 J/kgK
Thermal conductivity	17.6 W/mK
Coefficient of thermal expansion	11.5 x10^{-6} m/mK
Young's modulus	210 GPa

After sampling, the filter with the collected particles was weighed on a KERN ABJ analytical balance with a resolution of 0.1 mg. The particle mass was determined from the difference between the filter mass before and after the sampling. The particle-loaded filters were then coated with a thin carbon layer using a Balzers SCD 050 device prior to microscopic examination. The particle morphology was analyzed using a field-emission scanning electron microscope (FEG-SEM, Thermo Fisher Scientific Quattro S), while the chemical composition was determined by energy-dispersive X-ray spectroscopy (EDXS) using an Ultim® Max detector. The acquired micrographs were processed using ImageJ software to determine the particle geometry and size. The particle size was expressed as an equivalent diameter determined from the acquired micrographs by image analysis in accordance with ISO 13322-1.[14]

Figure 1: ZAMBELLI EGO PLUS TT personal sampler with associated sampling equipment

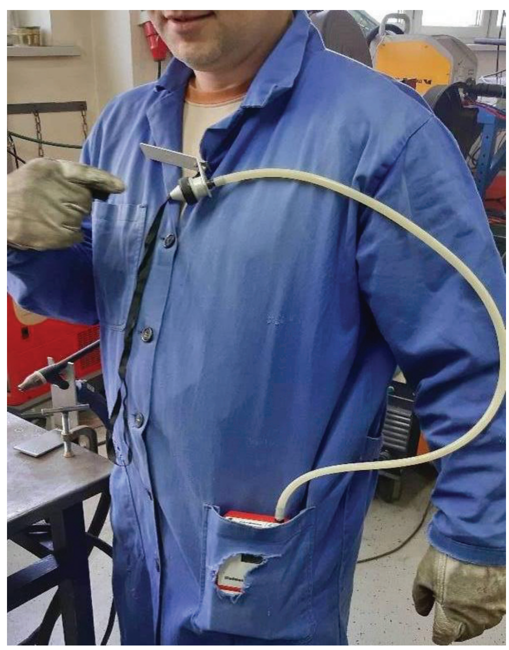

Figure 2: Position of the personal sampler in the operator's breathing zone

The oxyfuel cutting of the S460 tool steel was carried out using a gk TIP200/A cutting torch with acetylene and oxygen. The plasma cutting of the S460 tool steel was carried out using a Lincoln Electric INVERTEC PC100 plasma cutter operated with a direct current and a three-phase voltage of 400 V. During both cutting operations, particulate emissions were sampled using personal sampling to assess the operator's direct exposure. The sampler inlet was positioned approximately 30 cm from the mouth, in the operator's breathing zone, as shown in **Figure 2**.

Before each measurement, the instrument was calibrated, the particle collection time was set, and the appropriate filter was selected. Room temperature, air velocity, and relative humidity were also recorded during particle sampling. The measurement conditions were kept constant for all the cutting operations. The room air temperature was 21.5 °C, the air velocity was 0 m/s, and the relative humidity was 45 %. The air-flow rate through the filter was set to 3 L/min to simulate operator breathing. A mixed cellulose ester (MCE) filter with a diameter of 25 mm and a pore size of 0.8 μm was used.

3 RESULTS

The measured particulate emissions showed that the oxyfuel cutting of S460 tool steel generated higher dust emissions than plasma cutting. Since the particle sampling was performed for 1 min, the measured values were recalculated to an equivalent hourly emission rate. The emission rate measured during oxyfuel cutting was 0.096 g/h, whereas the corresponding value for plasma cutting was 0.066 g/h. Under the investigated conditions, the oxyfuel cutting therefore produced approximately 45 % higher particulate emissions than plasma cutting. **Figure 3** shows representative FEG-SEM micrographs of particles collected during the oxyfuel and plasma cutting of S460 tool steel.

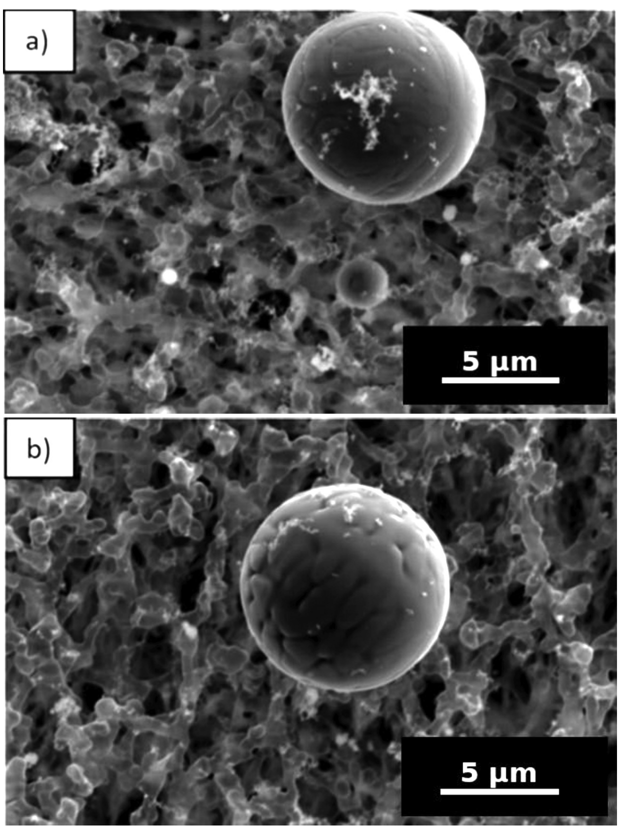

Figure 3: Representative FEG-SEM micrographs of particles collected during oxyfuel and plasma cutting of S460 tool steel: a) oxyfuel cutting; b) plasma cutting

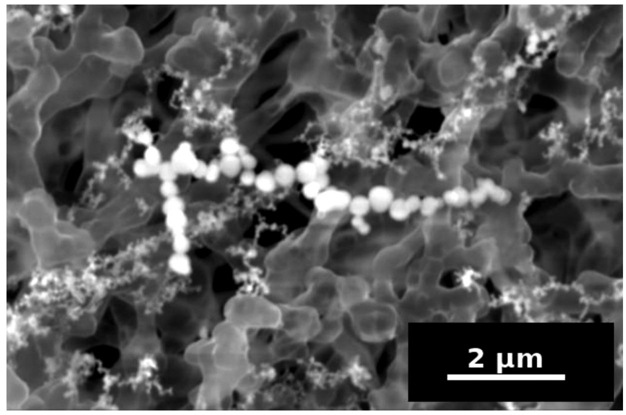

Figure 4: Cluster of fine particles collected during oxyfuel cutting of S460 tool steel

Analysis of the acquired micrographs showed that, in both cutting processes, most individual particles exhibited a predominantly spherical morphology. In addition to individual particles, particle clusters or agglomerates composed of multiple spherical particles were also observed. A representative cluster of fine particles collected during the oxyfuel cutting is shown in **Figure 4**.

Figure 5 shows the particle-size distribution for particles collected during the oxyfuel and plasma cutting of the S460 tool steel. The oxyfuel cutting produced a higher fraction of particles with an equivalent diameter below 1.75 μm, whereas the plasma cutting generated particles with diameters greater than 5.5 μm, which were not observed in the case of oxyfuel cutting. These results indicate that, on average, smaller particles were generated during oxyfuel cutting than during plasma cutting. All the analyzed particles collected during both cutting processes had diameters below 10 μm, indicating that they belong to the respirable particle size range and may reach the lower parts of the respiratory tract.

Figure 6 shows the elemental composition of particles collected on the filter during the oxyfuel cutting of S460 tool steel. Oxygen, chromium, silicon, iron, aluminum, manganese and nickel were detected in the analyzed particle agglomerates. The carbon signal was mainly associated with the mixed cellulose ester filter and the carbon coating applied prior to microscopic examination. Potassium was more pronounced in the filter background than in the particle agglomerates and was therefore not considered a reliable constituent of the ana-

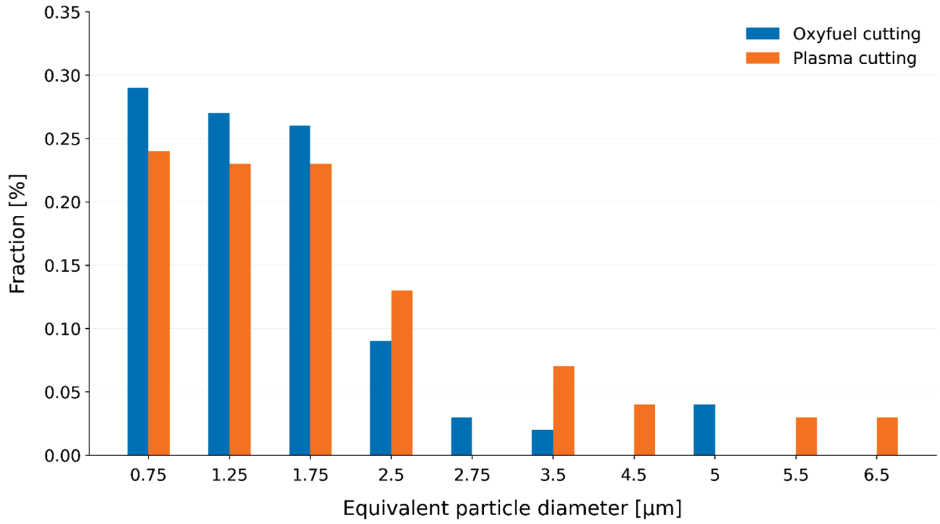

Figure 5: Particle-size distribution of particles collected during oxyfuel and plasma cutting of S460 tool steel as a function of equivalent particle diameter

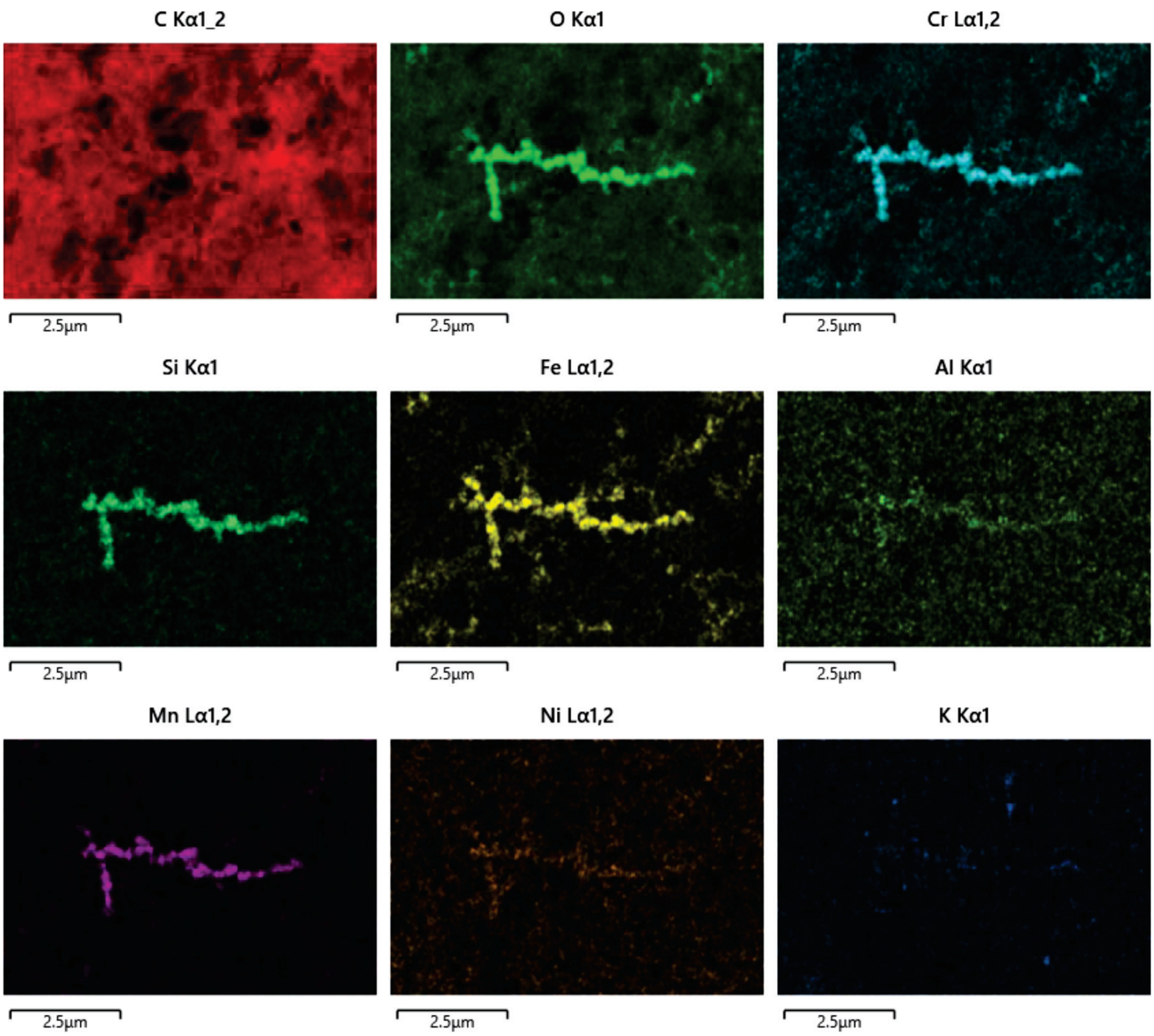

Figure 6: EDXS elemental maps of particles collected on the filter during oxyfuel cutting of S460 tool steel

lyzed particles. The elemental maps indicate that the detected metallic elements were spatially associated with the analyzed particle agglomerates.

4 DISCUSSION

The observed particle morphology can be explained by the mechanism of particle formation during thermal cutting. The emitted particles originated from the molten material and/or the condensed metal vapors generated in the cutting zone. During solidification, surface-tension effects favored the formation of predominantly spherical particles.[16] In addition to individual particles, agglomerates were also observed. Such agglomerates are commonly formed during the thermal processing of metals and may consist of smaller primary particles formed by condensation and collisions in the hot gas stream. Similar oxide-rich agglomerates have also been reported for thermally generated metal emissions.[5,6,9,10,16]

The particle-size analysis showed that the two cutting processes generated particulate matter with different size characteristics. The oxyfuel cutting produced a larger fraction of finer particles, whereas the plasma cutting generated a relatively greater proportion of larger particles. Since all analyzed particles were smaller than 10 µm, both cutting processes may contribute to operator exposure because such particles can penetrate the lower respiratory tract.[7,17] These process-dependent differences are consistent with previous studies showing that thermally generated metal emissions may vary substantially depending on the cutting process and operating conditions.[5,9,18–20] Taken together, the higher emission rate and the higher fraction of finer particles indicate that, under the investigated conditions, oxyfuel cutting represented the more intensive source of fine particulate emissions.

The elemental analysis revealed the presence of oxygen together with chromium, silicon, aluminum, iron, nickel, and manganese in the analyzed particle agglomerates. These elements correspond to both the base material and oxidation products formed during thermal cutting. Carbon signals were also detected; however, these were attributed primarily to the mixed cellulose ester filter and the carbon coating applied prior to SEM/EDXS examination. Potassium signals were observed predominantly in the filter background and were therefore not interpreted as a reliable constituent of the analyzed particles. The presence of oxygen suggests that part of the collected particulate matter consisted of oxidized metal particles formed during the thermal cutting.

The differences observed in filter masses before sampling indicate some variability in the initial filter condition. Since mixed cellulose ester filters are hygroscopic, they may absorb moisture from the surrounding air, which can influence the apparent filter mass and affect the gravimetric measurements. Filters should therefore be protected from ambient humidity and, if necessary, conditioned before use to minimize this effect.[12]

Because the particle volume increases with particle size, larger particles may contribute more substantially to the collected mass than finer particles, even when finer particles are more numerous in some size classes.[11] Particle size distributions should therefore be interpreted with caution when compared with gravimetric measurements. Image-based analysis reflects the particles visible in the acquired micrographs, whereas gravimetric weighing reflects the total particulate mass collected on the filter.[11,14,21] Consequently, image-based analysis may underestimate the total collected mass.

Besides their relevance to operator exposure, particulate emissions generated during thermal cutting should also be considered from a broader environmental perspective, since metal-containing particles may disperse into the surrounding environment and contribute to airborne particulate pollution.[22] However, the present study was conducted under controlled laboratory conditions and over a limited sampling period; therefore, the reported emission rates should be regarded as indicative only for the investigated cutting conditions. Further studies involving longer sampling periods and different cutting regimes would enable a more comprehensive assessment of particulate emissions and their potential environmental impact during thermal cutting.

5 CONCLUSIONS

The oxyfuel and plasma cutting of S460 tool steel generated respirable particulate emissions that differed in both quantity and size distribution. Under the investigated conditions, oxyfuel cutting produced higher particulate emissions than plasma cutting (0.096 g/h vs. 0.066 g/h) and generated a higher fraction of particles below 1.75 µm, whereas plasma cutting produced larger particles above 5.5 µm. All the analyzed particles were smaller than 10 µm, indicating their potential to penetrate the lower respiratory tract and contribute to operator exposure. EDXS analysis showed that the particles mainly contained oxygen together with iron, chromium, silicon, aluminum, nickel, and manganese, indicating the formation of oxidized metal particles during thermal cutting. Overall, oxyfuel cutting was identified as the more intensive source of fine particulate emissions.

6 REFERENCES

[1] D. Krajcarz, Comparison Metal Water Jet Cutting with Laser and Plasma Cutting, Procedia Engineering, 6 (**2014**), 838–843, doi:10.1016/j.proeng.2014.03.061

[2] M. F. Ashby, H. Shercliff, D. Cebon, Materials: Engineering, Science, Processing and Design, 4th ed., Butterworth-Heinemann, U.K., 2018, 303–406

[3] M. A. Wahab, Comprehensive Materials Processing, Elsevier Ltd., 6 (**2014**), 49–76

[4] M. Ilić, B. Kosec, Z. Čepić, B. Agarski, Z. Mirosavljević, Investigation of inhalable particles characteristics generated during welding of the stainless steel, Annals of the Faculty of Engineering Hunedoara, 18 (**2020**) 1, 19–24

[5] S. Eriksen Hammer, J. Ø. Halvorsen, P. Graff, T. K. Ervik, Characterisation of particles emitted during laser cutting of various metal sheets and an exposure assessment for the laser operators, International Journal of Environmental Research and Public Health, 19 (**2022**), 9888, doi:10.3390/ijerph19169888

[6] J. Wang, M. R. Short, M. T. D. McDonald, R. J. Burch, Characterization of particulate fume and oxides emission from stainless steel plasma cutting, Annals of Work Exposures and Health, 61 (**2017**) 3, 311–322

[7] S. A. Gunbeyaz, G. Akyuz, M. K. Kahveci, Workers' exposure to dust and potentially toxic elements during steel cutting in two ship dismantling cases, Ocean Engineering, 277 (**2023**), 114290

[8] J. M. Antonini, Health effects of welding, Critical Reviews in Toxicology, 33 (**2003**) 1, 61–103, doi:10.1080/713611032

[9] Y. Zhang, C. He, L. Morawska, Characteristics of airborne particles emitted during thermal cutting of metals, Journal of Cleaner Production, 336 (**2022**), 130401, doi:10.1016/j.jclepro.2022.130401

[10] N. Paulin, R. Pernetti, E. Bergamaschi, E. Oddone, Nanoparticles released during metal-processing operations: A systematic review, Cleaner Engineering and Technology, 24 (**2025**), 100873, doi:10.1016/j.clet.2024.100873

[11] M. Ilić, I. Budak, M. Vučinić-Vasić, A. Nagode, U. Kozmidis Luburić, J. Hodolič, T. Puškar, Size and shape particle analysis by applying image analysis and laser diffraction: inhalable dust in a dental laboratory, Measurement, 66 (**2015**), 109–117, doi:10.1016/j.measurement.2015.01.028

[12] MDHS, General methods for sampling and gravimetric analysis of respirable and inhalable dust, Health and Safety Executive, London, 2014

[13] E.-J. Ha, J.-H. Park, Analysis of deposited dust particles using SEM/EDX, Journal of Environmental Science International, 30 (**2021**) 3, 279–287, doi:10.5322/JESI.2021.30.3.279

[14] ISO 13322-1 (2014), Particle size analysis – Image analysis methods – Part 1: Static image analysis methods, International Organization for Standardization

[15] W. Yang, J. Ock, K. Kim, S. Park, N. Chae, H. Kim, K. Park, M.-H. Lee, S. Choi, Nano-to-micro aerosol contaminants emissions from dismantling of nuclear reactor pressure vessel using mock-up experiments, Nuclear Engineering and Technology, 58 (**2026**) 4, 104081, doi:10.1016/j.net.2025.104081

[16] A. Zimmer, P. Biswas, Characterization of the aerosols resulting from arc welding processes, Journal of Aerosol Science, 32 (**2001**) 8, 993–1008, doi:10.1016/S0021-8502(01)00014-3

[17] World Health Organization, Health effects of particulate matter, WHO Regional Office for Europe, Copenhagen, 2013

[18] M. Ilić Mićunović, R. Milošević, B. Kosec, A. Nagode, M. Ilić, Z. Tanasić, D. Klobčar, Investigation of the geometric characteristics of inhalable dust particles in a grinding process, Applied Sciences, 14 (**2024**), 5169, doi:10.3390/app14125169

[19] M.-H. Lee, W. Yang, N. Chae, S. Choi, High resolution size characterization of particulate contaminants for radioactive metal waste treatment, Nuclear Engineering and Technology, 53 (**2021**) 7, 2277–2288, doi:10.1016/j.net.2021.01.029

[20] K. O'Neill, X. Niu, J. Wang, R. Fang, Respirable particles and gas contaminants emissions from a desktop laser cutter and engraver, Aerosol and Air Quality Research, 24 (**2024**), 240032, doi:10.4209/aaqr.240032

[21] M. Elmes, M. Gasparon, Sampling and single particle analysis for the chemical characterisation of fine atmospheric particulates: A review, Journal of Environmental Management, 202 (**2017**), 137–150, doi:10.1016/j.jenvman.2017.07.041

[22] B. Agarski, I. Budak, B. Kosec, J. Hodolič, An approach to multi-criteria environmental evaluation with multiple weight assignment, Environmental Modeling & Assessment, 17 (**2012**) 3, 255–266, doi:10.1007/s10666-011-9294-y